ACS Catalysis

pubs.acs.org/acscatalysis
Research Article

Biochemical and Structural Characterization of $OvoA_{Th2}$: A Mononuclear Nonheme Iron Enzyme from *Hydrogenimonas thermophila* for Ovothiol Biosynthesis

Xinye Wang,[#] Sha Hu,[#] Jun Wang,[#] Tao Zhang,[#] Ke Ye, Aiwen Wen, Guoliang Zhu, Arturo Vegas, Lixin Zhang,* Wupeng Yan,* Xueting Liu,* and Pinghua Liu*

Cite This: *ACS Catal.* 2023, 13, 15417−15426
Read Online

ACCESS | Metrics & More | Article Recommendations | Supporting Information

ABSTRACT: Ovothiol A and ergothioneine are thiol-histidine derivatives with sulfur substitutions at the δ-carbon or ε-carbon of the L-histidine imidazole ring, respectively. Both ovothiol A and ergothioneine have protective effects on many aging-related diseases, and the sulfur substitution plays a key role in determining their chemical and biological properties, while factors governing sulfur incorporation regioselectivities in ovothiol and ergothioneine biosynthesis in the corresponding enzymes (OvoA, Egt1, or EgtB) are not yet known. In this study, we have successfully obtained the first OvoA crystal structure, which provides critical information to explain their C−S bond formation regioselectivity. Furthermore, $OvoA_{Th2}$ exhibits several additional activities: (1) ergothioneine sulfoxide synthase activity akin to Egt1 in ergothioneine biosynthesis; (2) cysteine dioxygenase activity using L-cysteine and L-histidine analogues as substrates; (3) cysteine dioxygenase activity upon mutation of an active site tyrosine residue (Y406). The structural insights and diverse chemistries demonstrated by $OvoA_{Th2}$ pave the way for future comprehensive structure−function correlation studies.

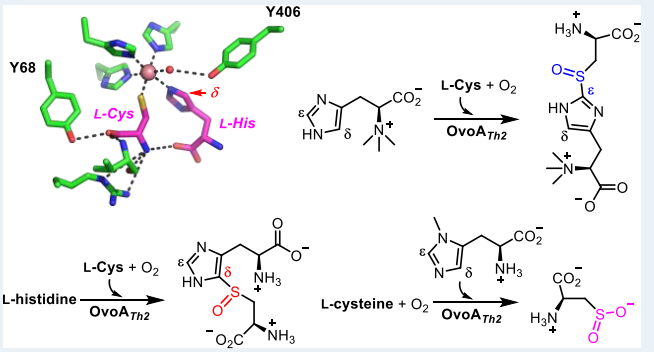

KEYWORDS: *nonheme iron enzyme, ovothiol, ergothioneine, X-ray structure, regioselectivity, sulfur-containing natural products*

INTRODUCTION

Ovothiol A (**1**) and ergothioneine (**2**) are naturally occurring thiol-histidine derivatives, featuring a sulfur substitution at the δ-carbon or the ε-carbon of their imidazole ring (Scheme 1),[1,2] respectively. The locations of the sulfur atom within the imidazole side-chain of ovothiol A **1** and ergothioneine **2** resulted in different physical and biological properties.[2] The pK_a of ovothiol's sulfur (∼1.4) is significantly more acidic than that of other natural thiols (usually falling within a range of 7.0 to 9.0).[2−6] Ovothiol A inhibits cell proliferation due to its activation of an autophagic process in human hepatocarcinoma cell lines, Hep-G2,[7] which indicates its potential anticancer activities. In contrast, ergothioneine is found primarily in its thiolate form under physiological conditions.[8,9] Ergothioneine's reduction potential (E_0' = −0.06 V)[6,10,11] is significantly higher than that of glutathione (E_0' = −0.25 V).[12] Ergothioneine can efficiently eradicate reactive oxygen species (ROS) and reactive nitrogen species (RNS).[13−15] Moreover, ergothioneine possesses protective effects in several human diseases, such as rheumatoid arthritis,[16,17] Crohn's disease,[18,19] neurodegenerative diseases,[20−23] cardiovascular disorders,[24] diabetes,[25] and fatty liver disease.[26,27] Ergothioneine may also cross the blood-brain barrier,[20−22] to protect against neurodegenerative diseases. Notably, Ames recently hypothesized that ergothioneine might be a longevity vitamin.[28]

Besides their biological activities, the biosynthetic and mechanistic characterization of sulfur-containing natural products has sparked new chemistries and enzymology.[29−32] While L-cysteine or methionine commonly serves as sulfur sources in sulfur-containing peptides, the realm of sulfur incorporation chemistry extends far beyond peptide-based natural products. Exemplifying this versatility is ovothiol A and ergothioneine biosynthesis, which present elegant instances across various facets,[1,30] encompassing sulfur sources, aerobic vs anaerobic biosynthetic routes, exploration of diverse catalytic strategies, meticulous control over sulfur-transfer regioselectivity, and notably, the shared and distinct features between sulfur and selenium chemistries.[33−36] Over the past

Received: August 25, 2023
Revised: October 27, 2023
Accepted: October 30, 2023
Published: November 14, 2023

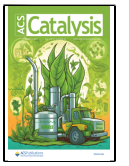

Scheme 1. Biosynthetic Pathways of Ergothioneine and Ovothiol A[a]

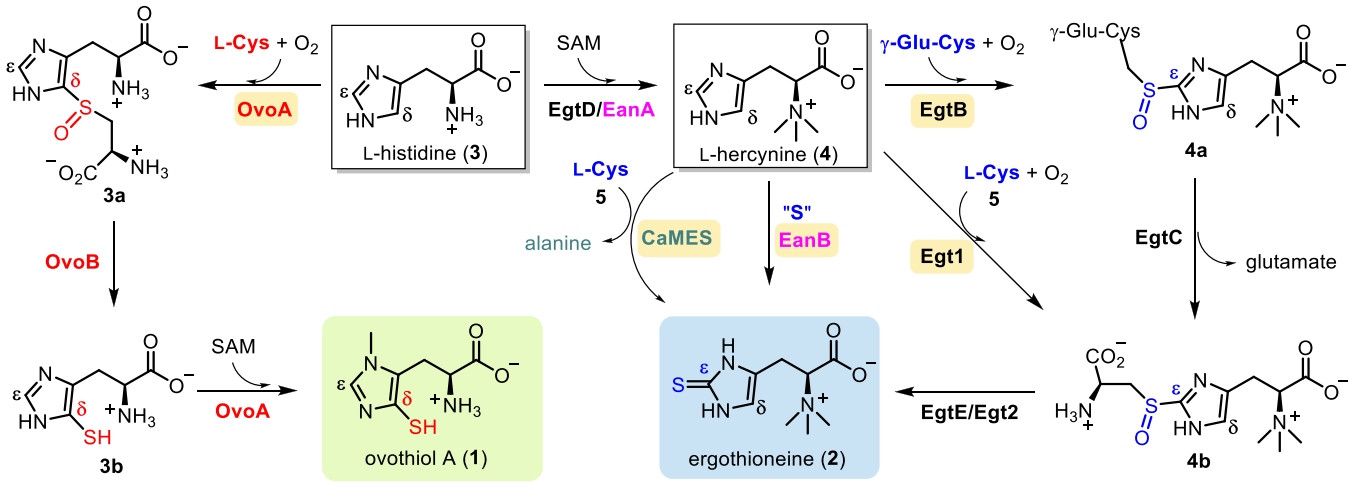

[a]The four ergothioneine biosynthetic routes are depicted on the right, while the aerobic ovothiol A biosynthetic pathway is illustrated on the left. Crucial C−S bond construction steps are catalyzed by EgtB, Egt1, EanB, CaMES, and OvoA, respectively.

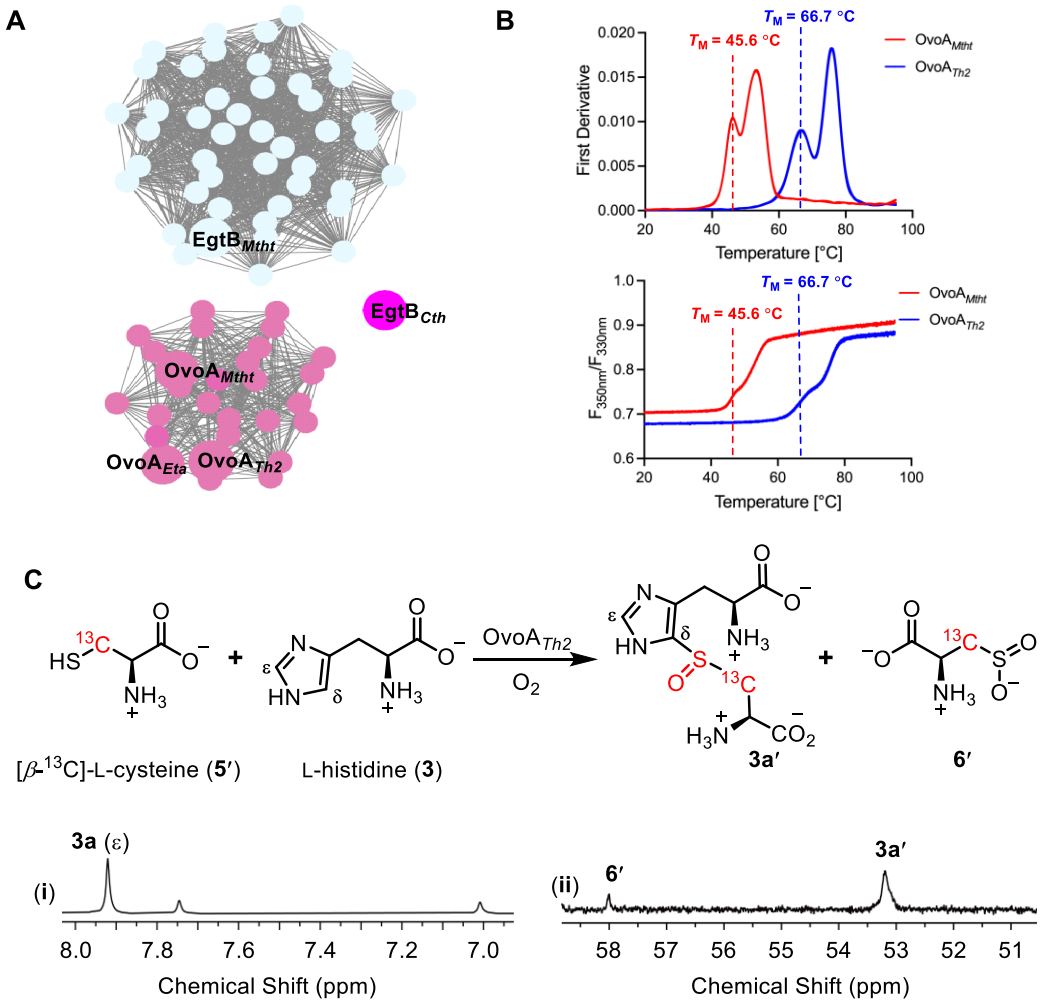

Figure 1. $OvoA_{Th2}$ characteristics. (A) Sequence similarity network analysis with an *E*-value of 10^{-60}, highlighting EgtB and OvoA nodes; (B) assessment of thermostability for $OvoA_{Mtht}$ and $OvoA_{Th2}$ via NanoDSF; (C) $OvoA_{Th2}$-catalyzed reactions using L-histidine and L-cysteine/[β-^{13}C]-L-cysteine substrates, obtained through ^{1}H NMR and ^{13}C NMR analysis.

decade, four biosynthetic pathways for ergothioneine and one for ovothiol A have been elucidated. In the two aerobic pathways leading to ergothioneine, namely the mycobacterial pathway (**4** → **4a** → **4b** → **2** transformations catalyzed by EgtB, EgtC, and EgtE enzymes, Scheme 1)[37,38] and the fungal *Neurospora crassa* pathway (**4** → **4b** → **2** transformations

https://doi.org/10.1021/acscatal.3c04026
ACS Catal. 2023, 13, 15417−15426

Table 1. Kinetic Parameters of Wild-Type OvoA$_{Th2}$ and Its Mutants under Different Conditions

enzyme	substrates	$k_{cat,\ O2}$ [min^{-1}]	$K_{M,\ L\text{-His or L-His derivatives}}$ [μM]	$K_{M,\ L\text{-Cys}}$ [μM]	k_{cat}/$K_{M,\ L\text{-His or L-His derivatives or L-Cys}}$ [min^{-1}μM^{-1}]	% of coupling product from NMR analysis
wild-type	L-His + L-Cys	589.0 ± 3.5	585.1 ± 28.0	278.6 ± 9.0	2.10 ± 0.09	~90%
wild-type	L-Her + L-Cys	127.2 ± 1.5	61.9 ± 3.5	(1.86 ± 0.04) E3	66.9 ± 2.3	~50%
wild-type	L-Cys	26.7 ± 0.4		(2.6 ± 0.2) E3		below the detection limit
wild-type	3-Me-L-His + L-Cys	131.2 ± 2.7	1.9 ± 0.1	252.2 ± 14.5	0.52 ± 0.04	below the detection limit
wild-type	1-Me-L-His + L-Cys	20.5 ± 0.3		(3.9 ± 0.1) E3	(5.3 ± 0.1) E-3	below the detection limit

enzyme	substrates	$k_{cat,\ O2}$ [min^{-1}]	$K_{M,\ L\text{-His}}$ [μM]	$K_{M,\ L\text{-Cys}}$ [μM]	$k_{cat}/K_{M,\ L\text{-Cys}}$ [min^{-1} μM^{-1}]	% of coupling product from NMR analysis
Y406F	L-His + L-Cys	361.2 ± 5.9	38.2 ± 2.6	575.2 ± 22.0	0.63 ± 0.09	~20%
Y68F	L-His + L-Cys	23.4 ± 0.2	50.9 ± 2.5	(61.9 ± 1.5) E3	(0.4 ± 0.1) E-3	~30%
Y68F/Y406F	L-His + L-Cys	14.8 ± 0.3	31.3 ± 4.0	(125.7 ± 11.0) E3	(1.2 ± 0.1) E-4	~10%

catalyzed by Egt1 & Egt2/EgtE enzymes, Scheme 1),[39,40] pivotal C−S bond formation steps are catalyzed by mononuclear nonheme iron enzymes. In particular, **4** → **4a** is catalyzed by EgtB, and **4** → **4b** is catalyzed by Egt1, using γ-glutamyl-cysteine (γ-GC)[37] or L-cysteine[39] as the sulfur sources, respectively. Subsequently, a PLP-dependent C−S lyase orchestrates the **4b** → **2** transformation catalyzed by either EgtE or Egt2 (Scheme 1), finalizing the sulfur transfer from L-cysteine to the L-histidine side-chain.[38,40] Recently, two anaerobic ergothioneine biosynthetic pathways have come to light. In the pathway of the green sulfur bacterium *Chlorobium limicola* (**3** → **4** → **2** transformations catalyzed by EanA-EanB catalysis, Scheme 1), the sulfur transfer is mediated by a rhodanese-domain-containing protein, EanB, utilizing polysulfide as the direct sulfur source and L-cysteine persulfide as an intermediate.[41,42] In the *Caldithrix abyssi* ergothioneine biosynthetic pathway of involving **3** → **4** → **2** transformations (Scheme 1), a molybdenum-containing enzyme, CaMES,[43] is responsible for the vital sulfur transfer step. While L-cysteine has been suggested as the sulfur source, the mechanistic intricacies of CaMES catalysis are yet to be thoroughly investigated. Currently, a solitary ovothiol A biosynthetic pathway has been characterized (**3** → **3a** → **3b** → **1** transformations catalyzed by OvoA and OvoB enzymes, Scheme 1).[44,45] In this ovothiol biosynthetic pathway, OvoA is a bifunctional enzyme encompassing sulfoxide synthase activity (**3** → **3a**, Scheme 1) and methyltransferase activity (**3b** → **1** transformations catalyzed by OvoA enzyme, Scheme 1).[44] Concurrently, OvoB serves as a PLP-dependent C−S lyase.[45]

Over the past decade, a pivotal query in the realm of ergothioneine and ovothiol biosynthetic research involves unraveling the factors that dictate the regioselectivity of these nonheme iron enzymes (EgtB/Egt1 vs OvoA).[46] Recently, two X-ray crystal structures of ergothioneine sulfoxide synthases, namely EgtB$_{Mthr}$[47] and EgtB$_{Cth}$,[48,49] have emerged. However, no crystal structure of the OvoA has been documented thus far. This report addresses this gap in knowledge by presenting the biochemical and structural insights of an ovothiol sulfoxide synthase, OvoA$_{Th2}$, derived from *Hydrogenimonas thermophila*. This is the first crystal structure of an ovothiol sulfoxide synthase.

RESULTS AND DISCUSSION

Identification of the Ovothiol Biosynthetic Enzymes Derived from a Thermophilic Organism, *H. thermophila*.

Due to the sulfur atom's importance in determining the chemical and biological properties of ovothiol A and ergothioneine, there has been extensive interest in uncovering the factors governing the sulfoxide synthase regioselectivities, i.e., OvoA vs EgtB/Egt1 selectivity.[46] The biochemically characterized OvoA isolated from *Erwinia tasmaniensis* (OvoA$_{Eta}$),[44,46,50,51] is very labile, and all crystallization efforts failed. Using OvoA$_{Eta}$ as the query sequence, we searched for the homologues in thermophiles or mesophilic microorganisms from UniProt and NCBI databases.[52] In total, 230 homologues were obtained. Using a protein sequence similarity network analysis approach, at an *E*-value cutoff of 10^{-60}, seventy-five representative sequences were categorized into two clusters (the EgtB branch and the OvoA branch), as well as a separate enzyme EgtB$_{Cth}$ carrying both Egt1 and EgtB activities (Figure 1A).[48,53] Among those sequences found within the OvoA node is the *H. thermophila* (WP_092912839) sequence was intriguing due to the optimal growth temperature of the microbe of approximately 55 °C.[54] This protein was subsequently named OvoA$_{Th2}$. Analysis of the protein domain organization of OvoA$_{Th2}$ suggests that similar to that of OvoA$_{Eta}$, OvoA$_{Th2}$ has both sulfoxide synthase and methyltransferase domains (Figure S1). Due to thermostability concerns in OvoA crystallization, after overexpression and purification of OvoA$_{Th2}$ (Figure S2) using a protocol similar to

https://doi.org/10.1021/acscatal.3c04026
ACS Catal. 2023, 13, 15417−15426

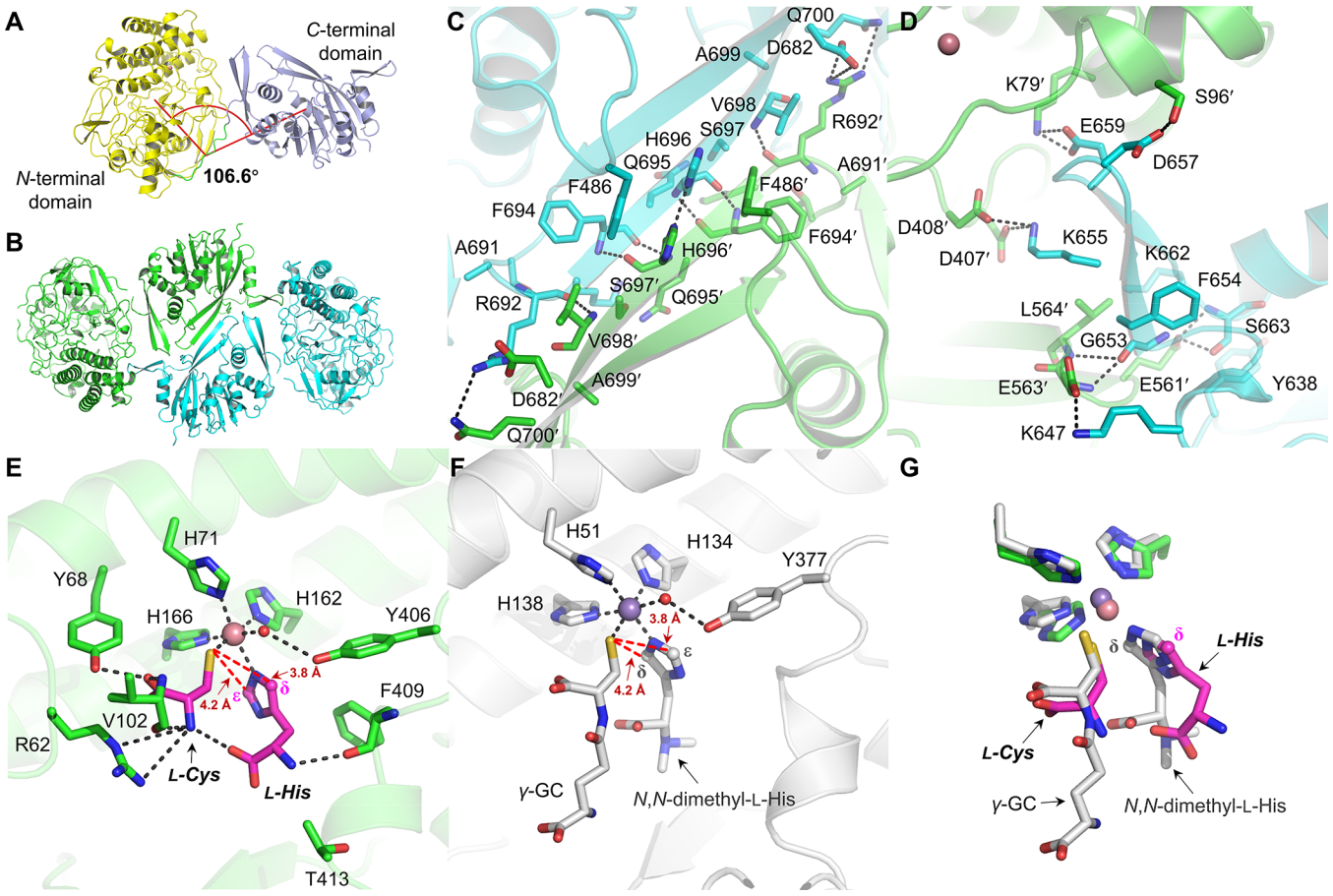

Figure 2. Crystal structure of OvoA$_{Th2}$. (A) Domain arrangement of OvoA$_{Th2}$. The OvoA·Co^{II}·L-Cys·L-His complex (PDB ID: 8KHQ) is shown in cartoon mode with yellow and light blue colors to present the *N*-terminal and *C*-terminal domains with a green linker, respectively. (B) Overall architecture of the OvoA$_{Th2}$ homodimer. The two monomers are colored green and cyan. (C and D) Dimer interfaces of OvoA$_{Th2}$. Each monomer was colored green and cyan, and the interacting residues were labeled with polar interactions highlighted in black dashes. (E) The active site of the OvoA·Co^{II}·L-Cys·L-His ternary complex. The residues around the active site in the *N*-terminal domain were shown as green sticks, while the metal cobalt as a pink sphere. (F) Active site of EgtB·Mn^{II}·γ-GC·*N*,*N*-dimethyl-L-His ternary complex (PDB ID: 4 × 8D).[47] The residues around the active site were shown as gray sticks, while the metal manganese as a sphere. (G) Superimposition between EgtB·Mn^{II}·γ-GC·*N*,*N*-dimethyl-L-His complex and OvoA·Co^{II}·L-Cys·L-His complex. The C$_\delta$ of the L-histidine imidazole ring was shown in sphere.

those employed for OvoA$_{Eta}$ and OvoA$_{Mtht}$ characterization,[46,52] we assessed the thermostability of OvoA$_{Th2}$ using a nanoDSF assay (Figure 1B).[55,56] The thermal unfolding curves of the peptide of OvoA$_{Mtht}$ are included for comparison purposes. Our analysis demonstrated that the T_M of OvoA$_{Th2}$ is approximately 21 °C higher than that of OvoA$_{Mtht}$ (Figure 1B).

Domain analysis of OvoA$_{Th2}$ suggested that it possesses an *N*-terminal formylglycine-generating enzyme (FGE) sulfatase domain as well as a *C*-terminal methyltransferase domain (Figure S1). OvoA$_{Eta}$ contains a similar domain organization, with our biochemical characterization supporting the bifunctionality of OvoA$_{Eta}$: ovothiol sulfoxide synthase and methyltransferase (Scheme 1).[45] OvoA$_{Th2}$ catalysis was analyzed using three different assays to provide evidence to support the activity of OvoA$_{Th2}$ as an ovothiol sulfoxide synthase (Figures 1C and S3): (a) ^{1}H NMR to examine the L-histidine imidazole side-chain for ovothiol sulfoxide synthase regioselectivity; (b) ^{13}C NMR assay for L-cysteine activities using [β-^{13}C]-L-cysteine as a substrate; (c) oxygen consumption rate analysis utilizing a Neo-Foxy oxygen electrode to assess the overall O_2 consumption rate.

In the ^{1}H NMR spectra, based on previously reported results pertaining to Egt1/EgtB/OvoA,[39,46,52] the ∼7.60 and 6.80 ppm peaks were assigned to L-histidine imidazole H$_\varepsilon$ and H$_\delta$, respectively. In the OvoA$_{Th2}$ catalyzed reaction, when L-histidine (**3**) and L-cysteine (**5**) were utilized as substrates, the product ^{1}H NMR signal was found to be ∼7.92 ppm (trace i, Figures 1C and S3), assigned to H$_\varepsilon$ based on prior studies on OvoA$_{Eta}$,[46] which suggests that OvoA$_{Th2}$ catalyzes sulfoxide formation at the δ-position, the ovothiol class of sulfoxide regioselectivity. In the ^{13}C NMR spectrum of the reaction mixture from the L-histidine and [β-^{13}C]-L-cysteine reaction, two signals at 58.0 and 53.2 ppm were observed (trace ii, Figure 1C). The 53.2 ppm signal is consistent with [β-^{13}C]-sulfoxide product **3a′** as reported in prior OvoA$_{Eta}$ studies.[52,57] The signal at 58.0 ppm is consistent with L-cysteine sulfinic acid,[57] while the level of [β-^{13}C]-L-cysteine sulfinic acid **6′** represents approximately ∼10% of the product mixture. Therefore, OvoA$_{Th2}$ indeed acts as an ovothiol sulfoxide synthase. The oxygen consumption assay using a NeoFoxy electrode indicated that the kinetic parameters of OvoA$_{Th2}$ using L-histidine and L-cysteine at 23 °C are $k_{cat,\ O2}$ = 589.0 ± 3.5 min^{-1}; $K_{M,\ L\text{-His}}$ = 585.1 ± 28.0 μM, and $K_{M,\ L\text{-cys}}$ = 278.6 ± 9.0 μM (Table 1 and Figure S4).

Overall Structure of OvoA$_{Th2}$. After demonstrating that OvoA$_{Th2}$ is the ovothiol sulfoxide synthase for ovothiol

https://doi.org/10.1021/acscatal.3c04026
ACS Catal. 2023, 13, 15417−15426

biosynthesis, we sought to crystallize it. Because $OvoA_{Th2}$'s thermal unfolding temperature T_M is ~21 °C higher than that of $OvoA_{Mtht}$ (Figure 1B), our crystallization efforts on $OvoA_{Th2}$ indeed were successful, obtaining the $OvoA_{Th2}$ crystal structure at a resolution of 2.7 Å in complex with its two substrates, L-histidine and L-cysteine (Figure 2, OvoA·Co^{II}·L-Cys·L-His, PDB ID: 8KHQ). $OvoA_{Th2}$ contains two functional domains: a sulfatase domain at the *N*-terminus (7−455) and a SAM-dependent methyltransferase domain at the *C*-terminus (466−707). Each domain forms a distinctive globular region, and these two domains are linked via a linker loop (456−465). The shaft angle between the mass centers of the two domains and the center of the linker is 106.6° (Figure 2A). Two $OvoA_{Th2}$ monomers dimerize through a 2-fold symmetry in which the two *C*-terminal methyl transferase domains are at the center, flanked by the two *N*-terminal domains on either side. Such an arrangement results in a flat, rhomboid-shaped structure with three nodes (dimer of *C*-terminal domains in the middle, two *N*-terminal domains on each side) (Figure 2B). Based on calculations using the PISA server,[58] the dimer interface of $OvoA_{Th2}$ is 1,951 $Å^2$, occupying approximately 6.5% of the total surface accessible area. Two $OvoA_{Th2}$ regions are responsible for the dimerization. The first region is a β-strand resulting from residues T690-Q700 at the *C*-terminus. The β-strands from the two monomers stack in an antiparallel manner. Moreover, salt bridges were observed to link R692 of one monomer to D682′ of the other monomer. The H696 residue forms a hydrogen bond with the same residue H696′ on the other monomer while interacting with F486′ through π stacking, which may help to orient the *C*-terminal domains (Figure 2C). The second monomer interface is primarily driven by the *C*-terminal domain of one monomer with the *N*-terminal domain of the other monomer. Residues G653-K662 form a short β-hairpin, which slots into the cavity built from N78′ to S100′ and I405′ to D408′ from the *N*-terminal domain of the other monomer (Figure 2D). The residues flanking this β-hairpin, (i.e., Y638−W650 and S663−D665) also participate in dimerization through interactions with the β-hairpin formed by T560′-L564′ in the other monomer. Apart from hydrophobic interactions, intensive polar interactions also occur, including salt bridging between K647:E563′, K655:D407′, K655:D408′, and E659:K79′, as well as hydrogen bonding between D657:S96′, S663:E561′, and G653:E563′, G653:L564′ (Figures 2D and S5).

Active Site Analysis of the $OvoA_{Th2}$·Co^{II}·L-Cys·L-His Ternary Complex. Upon cocrystallization of $OvoA_{Th2}$ with its substrates, L-cysteine and L-histidine, we mixed apo $OvoA_{Th2}$, Co^{II}, L-Cys, and L-His in a molar ratio of 1:3:3:3 and successfully solved the structure of $OvoA_{Th2}$·Co^{II}·L-Cys·L-His complex, which was crystallized anaerobically in an anaerobic Coy-chamber to avoid transformations during the crystallization process (Figures 2E and S6). The metallo-center is coordinated by three L-histidine residues (H71, H162, and H166). The L-histidine substrate coordinates to Co^{II} *trans* to H71 using the imidazole *N*1 atom, and the L-cysteine substrate is *trans* to H162. The sixth coordination site is occupied by a water molecule (outlined in chain B), which is a potential oxygen-binding site. A conserved tyrosine residue (Y406) forms a hydrogen bond with the coordinating water at a distance of 3.1 Å (visible in chain B, Figure 2E). The L-cysteine substrate is also involved in a hydrogen bonding network involving R62, Y68, the backbone of V102, and the carboxyl group of the L-histidine substrate. Apart from interactions with the L-cysteine substrate, the L-histidine substrate also interacts with the F409 backbone by hydrogen bonds, and a portion of L-histidine is also close to Y406 as well as the nonpolar portion of T413 through nonpolar contacts (Figure 2E).

To examine structural factors crucial for the sulfoxide formation regioselectivity in $OvoA_{Th2}$ relative to ergothioneine sulfoxide synthase (Egt1 or EgtB), we focused on the $OvoA_{Th2}$*N*-terminal domain as it is the sulfoxide synthase domain. EgtB from *Mycobacterium thermophilum* ($EgtB_{Mthr}$, PDB ID: 4 × 8D)[47,49] possesses the highest structural similarity to $OvoA_{Th2}$, with an RMSD of 2.3 Å. $EgtB_{Mthr}$ uses *N*,*N*,*N*-trimethyl-histidine (L-hercynine) and γ-glutamyl-cysteine (γ-GC) as substrates (Scheme 1).[37,47,59] Both ergothioneine and ovothiol sulfoxide metallo-centers are coordinated by four imidazoles of L-histidine/hercynine residues (three L-histidine residues from the protein and one from the L-histidine/hercynine substrate) and one L-cysteine, leaving an additional site unoccupied for O_2 binding and activation. Seebeck and co-workers successfully solved the crystal structure of $EgtB_{Mthr}$·Mn^{II}·γ-GC·*N*,*N*-dimethyl-L-histidine complexes (Figure 2F).[47] In the $OvoA_{Th2}$·Co^{II}·L-Cys·L-His and $EgtB_{Mthr}$·Mn^{II}·γ-GC·*N*,*N*-dimethyl-L-histidine complexes (Figure 2G), the L-cysteine portions possess a similar orientation. Interestingly, the imidazole of the *N*,*N*-dimethyl-L-histidine in the $EgtB_{Mthr}$·Mn^{II}·γ-GC·*N*,*N*-dimethyl-L-histidine complexes flips approximately 180° relative to the L-histidine in the $OvoA_{Th2}$·Co^{II}·L-Cys·L-His complex. Such differences expose the L-histidine C_δ to the L-cysteine sulfur atom in the $OvoA_{Th2}$·Co^{II}·L-Cys·L-His complex, while in the $EgtB_{Mthr}$·Mn^{II}·γ-GC·*N*,*N*-dimethyl-L-histidine complex, the C_ε position in *N*,*N*-dimethyl-L-histidine is closer to the cysteine sulfur atom in γ-GC (Figure 2G). In our prior biochemical characterizations, we have demonstrated that the use of *N*,*N*-dimethyl-L-histidine and L-hercynine as $OvoA_{Eta}$ substrates result in the same sulfoxide synthase regioselectivity, the ergothioneine type.[46] Therefore, this comparative structural analysis suggests that the relative orientation of the L-histidine imidazole side-chain in the enzyme active site determines the ovothiol and ergothioneine sulfoxide synthase regioselectivities.

The largest difference between the active site of $OvoA_{Th2}$ and $EgtB_{Mthr}$ is a loop region (residues 98 to 117 in $OvoA_{Th2}$ vs residues 80−95 in $EgtB_{Mthr}$), acting as a lid to cover the subpocket for the L-cysteine substrate. In $EgtB_{Mthr}$, this loop region flips toward the solvent (Figure S7). We proposed that this loop region modulates the substrate preference in this family of sulfoxide synthases, where the relatively smaller subpocket in OvoA covered by this loop could accommodate only L-cysteine as the sulfur donor. At the same time, the more spacious pocket in $EgtB_{Mthr}$ could accommodate γ-GC as the sulfur donor. Similar conclusions can also be drawn from the comparison of the crystal structure of $EgtB_{Cth}$ from *Chloracidobacterium thermophilum* to $OvoA_{Th2}$.[48,49] Residues 91 to 111 in $EgtB_{Cth}$ represent the loop serving as the lid for covering the subpocket.

In $EgtB_{Mthr}$, a tyrosine residue (Y377) has been proposed to be critical to the sulfoxide synthetase activity.[47] In $EgtB_{Cth}$,[48,49] two tyrosine residues (Y92 and Y93) are catalytically important. In $OvoA_{Th2}$, there is a conserved tyrosine residue (Y406) in the same position relative to Y337 in $EgtB_{Mthr}$. Given the similarity between $OvoA_{Th2}$ and $EgtB_{Mthr}$, Y406 in $OvoA_{Th2}$ may be critical for ovothiol sulfoxide synthase activity.

Functional Diversities of $OvoA_{Th2}$ Derived from *H. thermophila*. In two OvoA enzymes reported in the literature

https://doi.org/10.1021/acscatal.3c04026
ACS Catal. 2023, 13, 15417−15426

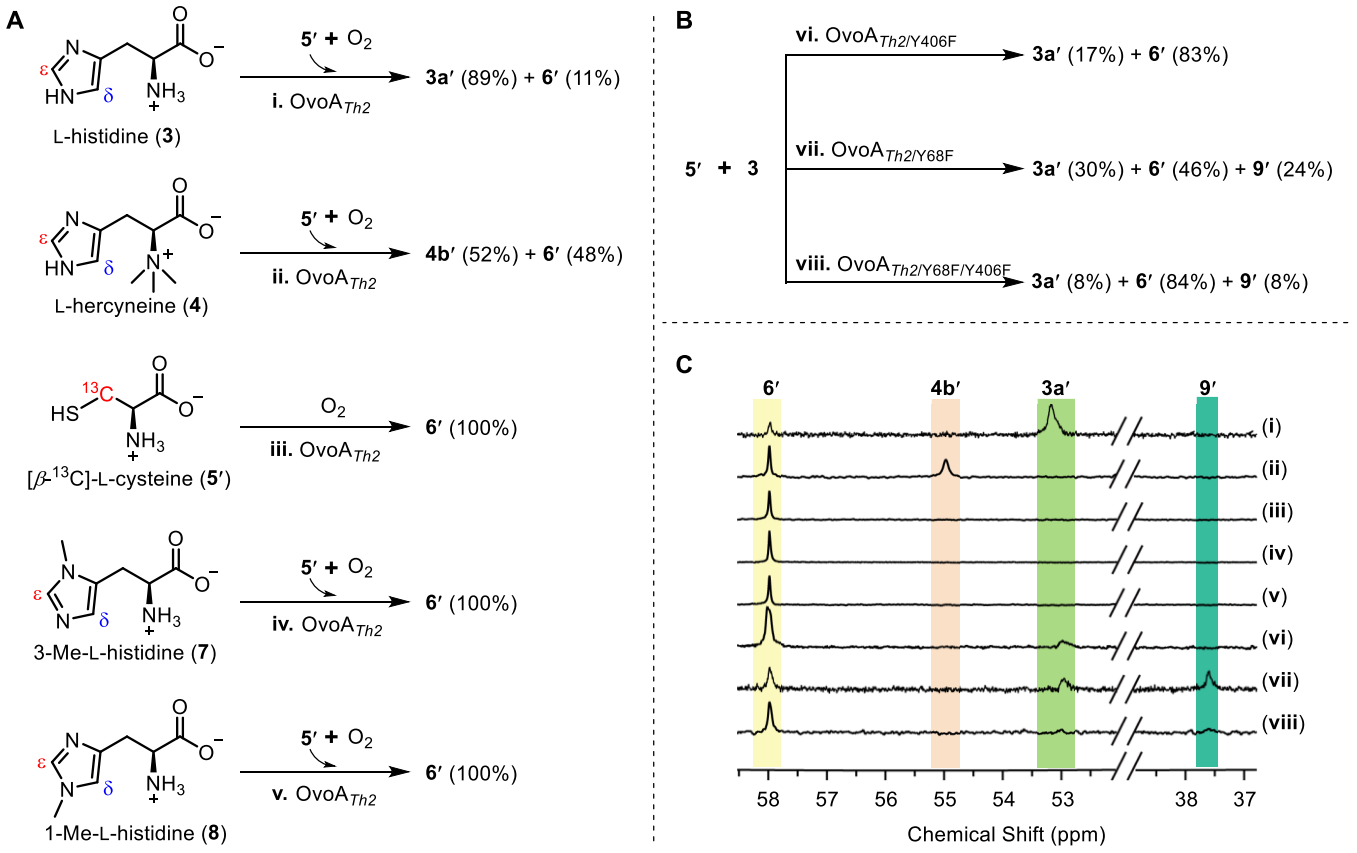

Figure 3. Characterization of OvoA$_{Th2}$ and its variants under a few different conditions. (A) Results of wild-type OvoA$_{Th2}$-catalyzed reactions using [β-^{13}C]-L-cysteine (**5′**) and L-histidine (**3**) or derivatives (L-hercynine (**4**), 3-methyl-L-histidine (**7**), and 1-methyl-L-histidine (**8**)) as substrates or using **5′** as the only substrate. (B) Evaluation of OvoA$_{Th2}$ variants OvoA$_{Th2/Y406F}$ and OvoA$_{Th2/Y68F}$ and its double mutant OvoA$_{Th2/Y68F/Y406F}$ for their relative sulfoxide and CDO-like synthase activity using **5′** and **3** as substrates. (C) ^{13}C NMR analysis of reactions: wild-type OvoA$_{Th2}$ using **5′** and **3** as substrates (i), OvoA$_{Th2}$ using **5′** and **4** as substrates (ii), OvoA$_{Th2}$ using **5′** as the only substrate (iii), OvoA$_{Th2}$ using **5′** and **7** as substrates (iv), OvoA$_{Th2}$ using **5′** and **8** as substrates (v), OvoA$_{Th2/Y406F}$ using **5′** and **3** as substrates (vi), OvoA$_{Th2/Y68F}$ using **5′** and **3** as substrates (vii), and OvoA$_{Th2/Y68F/Y406F}$ using **5′** and **3** as substrates (viii).

(OvoA$_{Eta}$[46,57,60] and OvoA$_{Mtht}$[52]), outside of the ovothiol sulfoxide synthase activities, under some conditions, these enzymes produce L-cysteine sulfinic acid as a dominant product, displaying cysteine dioxygenase (CDO) activity. The partitioning between CDO and ovothiol sulfoxide synthase activities can be tuned through metallo-center ligands or by the secondary coordination shell residues. Critically, both OvoA$_{Eta}$ and OvoA$_{Mtht}$ have ergothioneine sulfoxide synthase activity when using L-hercynine and L-cysteine as substrates.[46,52] In the previous section, we summarized the crystal structure data from OvoA$_{Th2}$. The next key point to be addressed is whether the unique biochemical properties reported in the literature for OvoA$_{Eta}$ and OvoA$_{Mtht}$ are common to OvoA$_{Th2}$. If OvoA$_{Th2}$ possesses the same properties, the structural information reported for OvoA$_{Th2}$ will be a solid foundation for future structure−function correlation studies.[61] To answer this question, we systematically characterized OvoA$_{Th2}$ reactivity under various conditions (Figure 3 and Table 1): (1) ovothiol vs ergothioneine sulfoxide synthase activity; (2) cysteine dioxygenase activity; (3) roles of active site tyrosine residues.

OvoA$_{Th2}$ is an ovothiol sulfoxide synthase (Figure 1). When [β-^{13}C]-cysteine was used to replace cysteine, it generated [β-^{13}C]-sulfoxide **3a′** as a major product and [β-^{13}C]-L-cysteine sulfinic acid **6′** as a minor product (~10% of the reaction mixture). Interestingly, OvoA$_{Th2}$ possesses ergothioneine sulfoxide synthase activity (Figure S8). Upon swapping in L-hercynine for L-histidine, ^{1}H NMR clearly indicated that OvoA$_{Th2}$ is an ergothioneine sulfoxide synthase, as demonstrated by the signal at 7.23 ppm in the ^{1}H NMR spectrum, which is the signal for the imidazole δ-position hydrogen atom (Figure S8). This result suggests sulfoxide formation at the L-hercynine ε-carbon. This conclusion was further supported by ^{13}C NMR analysis of the reaction using L-hercynine and [β-^{13}C]-L-cysteine as substrates. In the ^{13}C NMR spectrum, the signal at 55.0 ppm was derived from [β-^{13}C]-sulfoxide **4b′**, and the signal at 58.0 ppm was derived from [β-^{13}C]-L-cysteine sulfinic acid **6′**. The ratio between **4b′** and **6′** is approximately 1:1 (trace ii, Figure 3). Kinetic analysis using an O_2 consumption assay demonstrated that the kinetic parameters for this reaction at 23 °C are $k_{cat,\ O2}$ = 127.2 ± 1.5 min^{-1} ; $K_{M,\ L\text{-}Her}$ = 61.9 ± 3.5 μM, and $K_{M,\ L\text{-}cys}$ = 1.86 ± 0.04 mM (Figure S9, Table 1). Clearly, upon changing L-histidine to L-hercynine, OvoA$_{Th2}$ makes a corresponding alteration in activity from an ovothiol sulfoxide synthase to an ergothioneine sulfoxide synthase. We measured the CDO activity of the molecule of OvoA$_{Th2}$ using L-cysteine as the substrate. The signal at 58.0 ppm in the ^{13}C NMR experiments did support the CDO activity when L-cysteine was the only substrate (trace iii, Figures 3and S10). The steady-state kinetics parameters are $K_{M,\ L\text{-}Cys}$ = 2.6 ± 0.2 mM, and a much lower $k_{cat,\ O2}$ = 26.7 ± 0.4 min^{-1} (Figure S11, Table 1).

https://doi.org/10.1021/acscatal.3c04026
ACS Catal. 2023, 13, 15417−15426

The alterations in activity upon the replacement of L-histidine with L-hercynine clearly suggest that the catalysis of $OvoA_{Th2}$ is sensitive to subtle modifications to the enzyme's active site. We examined two additional histidine analogs, 3-methyl-L-histidine (**7**) and 1-methyl-L-histidine (**8**), which have the two imidazole nitrogen atoms methylated, respectively. Using 3-methyl-L-histidine (**7**) and L-cysteine as substrates, only [β-^{13}C]-L-cysteine sulfinic acid **6′** (δ_C 58.0) was observed as a product (trace iv, Figures 3 and S12−S13, Table 1) with the $k_{cat,\ O2}$ = 131.2 ± 2.7 min^{-1}. Similar results were also observed when 1-methyl-L-histidine (**8**) and L-cysteine were used as substrates (trace v, Figures 3 and S14, Table 1), producing only [β-^{13}C]-L-cysteine sulfinic acid **6′** with $k_{cat,\ O2}$ = 20.5 ± 0.3 min^{-1} (Figure S15).

Results from the above experiments demonstrated that the activities of the $OvoA_{Th2}$ can be tuned across ovothiol sulfoxide synthase, ergothioneine sulfoxide synthase, and CDO activities. When L-histidine and L-cysteine were substrates, ∼90% of the product in the reaction mixture was found to be sulfoxide **3a**. However, in the case of L-hercynine and L-cysteine reactions, ergothioneine sulfoxide **4b** and L-cysteine sulfinic acid **6** are produced at comparable levels. In the cases of both 3-methyl-L-histidine and 1-methyl-L-histidine, $OvoA_{Th2}$ displays CDO activity, with reduced k_{cat} values by ∼4.5 and 28.7-fold, respectively (Table 1).

In the structure of the $OvoA_{Th2}$·Co^{II}·L-Cys·L-His complex, two tyrosine residues, Y68 and Y406, are close to the metallocenter and substrate binding site. It has been identified that active site tyrosine residues are critical to ovothiol and ergothioneine sulfoxide synthase activity.[48−52,60] We, therefore, characterized the phenylalanine mutants of these two tyrosine residues. Three mutants have been biochemically and kinetically analyzed, including Y68F and Y406F single mutants and the Y68F/Y406F double mutant of $OvoA_{Th2}$. The kinetic parameters of these mutants are summarized in Table 1.

In the Y406F mutant, the kinetic parameters were measured through an O_2 consumption assay at 23 °C (Table 1 and Figures S16−S17). In comparison to the parameters obtained for wild-type $OvoA_{Th2}$, $OvoA_{Th2/Y406F}$ has a K_M for the L-histidine substrate decreased by 15-fold from 585.1 ± 28.0 μM in wild-type $OvoA_{Th2}$ to 38.2 ± 2.6 μM, while their k_{cat}s are comparable. The product analysis of the Y406F reaction determined that the dominant product (>80%) of the Y406F mutant reaction is [β-^{13}C]-L-cysteine sulfinic acid **6′**, with a small amount of [β-^{13}C]-sulfoxide **3a′** representing ∼20% of the product mixture (trace vi, Figure 3). In the Y68F mutant, the results differ from both the wild-type and Y406F mutant (Table 1 and Figures S18−S19). Compared to the parameters of the wild-type $OvoA_{Th2}$, the K_M for the L-cysteine substrate increases by nearly 200-fold, and the $k_{cat,\ O2}$ decreased by approximately 25-fold for $OvoA_{Th2/Y68F}$. As a result, in the $OvoA_{Th2}$ Y68F mutant, the catalytic efficiency ($k_{cat}/K_{M,\ L\text{-}Cys}$) decreases by nearly 5.5 × 10^3-fold. ^{1}H NMR and ^{13}C NMR analysis of the Y68F mutant reaction demonstrated that the product ratio of [β-^{13}C]-sulfoxide **3a′**, [β-^{13}C]-L-cysteine sulfinic acid **6′**, and [β-^{13}C]-L-cystine **9′** is approximately 5:3:2 (trace vii, Figures 3 and S18). Based on the crystal structure depicted in Figure 2, Y68 directly interacts with the carboxylate of the L-cysteine substrate through hydrogen bonding. In the double mutant variant Y68F/Y406F, the kinetic parameters are comparable to those of the Y68F mutant. However, ^{1}H NMR and ^{13}C NMR analysis suggested that the double mutant variant produces L-cysteine sulfinic acid as the dominant product, while sulfoxide and cystine are below the detection levels (Table 1, trace viii in Figures 3 and S20−21). Therefore, with the use of 3-methyl-L-histidine and 1-methyl-L-histidine as the substrate or by using the Y68F/Y406F mutant, $OvoA_{Th2}$ exhibits predominantly the CDO activity rather than an ovothiol sulfoxide synthase activity. Such flexibility in the $OvoA_{Th2}$ activities suggests it is an excellent platform for future structure−function relationship studies.

CONCLUSIONS

Sulfur is one of the most abundant elements in the natural world. In recent years, an interdisciplinary approach has been employed to characterize sulfur incorporation chemistry,[30] encompassing biosynthetic sulfur sources, intermediates, and, notably, mechanistic insights into new strategies for sulfur-related biosynthetic pathways. With the exponential expansion of microbial genomes accessible through public databases,[62] new biosynthetic and mechanistic knowledge has been harnessed in genome mining initiatives to systematically identify related natural products and their underlying biosynthetic routes. In the biosynthesis of sulfur-containing natural products, L-cysteine, or its derivatives (e.g., glutathione and mycothiol), have conventionally served as direct sulfur sources. Recent instances include the use of thiocysteine in leinamycin biosynthesis[63] and the utilization of polysulfide in a specific anaerobic ergothioneine biosynthetic pathway.[41,42] In numerous other cases, the precise sulfur sources remain unidentified and are simply denoted as "S".[1,29,30,61]

Mechanistically, sulfur transfer chemistry can be accomplished through nucleophilic substitution or radical mechanisms. For nucleophilic substitution chemistry, the two common intermediates are thiocarboxylate or L-cysteine persulfide on carrier proteins, as evidenced in biosynthetic studies of BE-7585A.[64] For sulfur carrier proteins generating thiocarboxylate intermediates, they terminate with a C-terminal Gly-Gly. Some exceptions to this general structural motif have been reported, in which the C-terminal Gly-Gly motif was released from the carrier protein after proteolysis through the removal of the C-terminal residues by a dedicated protease.[65,66] Recently, persulfides and thiocarboxylates have been implicated as key intermediates in the biosynthesis of thioamides, functional groups in sulfur-modified tRNA, and many small molecular natural products.[31] Similar to thiazoline/thiazole in peptide-based natural products,[67] thioamide generation is generally an ATP-dependent process involving either phosphorylation or adenosylation activation[32] and L-cysteine, protein-bound thiocarboxylates, or L-cysteine persulfides have been suggested as sulfur sources, while in many cases, the sulfur sources are unknown.[31]

In addition to these novel sulfur natural product biosynthetic examples, ergothioneine and ovothiol A biosynthesis represent exceptional examples (Scheme 1). Their important biological properties are consistent with the use of several different strategies to produce these two compounds.[28] Both aerobic and anaerobic biosynthetic pathways involving sulfur's nucleophilic chemistries[41−43] and radical chemistries[1] have been reported for ergothioneine biosynthesis. For the aerobic ergothioneine and ovothiol A biosynthetic pathways, the crucial transformation is the nonheme iron enzyme-catalyzed sulfoxide formation reactions (EgtB, Egt1, and OvoA). One of the most important mechanistic questions is how these enzymes modulate the sulfoxide formation regioselectivities

https://doi.org/10.1021/acscatal.3c04026
ACS Catal. 2023, 13, 15417−15426

(Scheme 1). Over the past decade, two X-ray crystal structures of ergothioneine sulfoxide synthases, namely $EgtB_{Mthr}$[47] and $EgtB_{Cth}$,[48,49] have been reported. However, due to thermostability issues faced in the OvoA studies, it has been difficult to obtain the ovothiol sulfoxide synthase structure. In this work, using enzymes with significantly improved thermostability (~21 °C increase in thermostability for $OvoA_{Th2}$ relative to $OvoA_{Mtht}$), we have obtained the first ovothiol sulfoxide synthase crystal structure. This paves the way for more detailed structure−function relationship studies.[61] More importantly, in spite of the low sequence homology (47.6% identity relative to $OvoA_{Mtht}$) and a significant increase in thermostability, $OvoA_{Th2}$ shares nearly all biochemical properties with $OvoA_{Mtht}$.[52] First, $OvoA_{Th2}$ possesses both ovothiol and ergothioneine sulfoxide synthase activities, and such tuning-in activities are controlled by the orientation of the imidazole side chain in the enzyme active site (Figure 2). Second, $OvoA_{Th2}$ has CDO activity, and the activities between CDO and sulfoxide synthase can be modulated using either substrate analogs (e.g., 3-methyl-L-histidine or 1-methyl-L-histidine) or by mutations in active site tyrosine residues (e.g., Y68F/Y406F double mutant). The structural information reported in this study and the rich chemistries displayed by $OvoA_{Th2}$ have laid a solid foundation for future structure−function correlation studies. This structural information may also assist future engineering efforts in obtaining enzymes that are more suitable for the production of ergothioneine and ovothiol in an industrial setting.[68]

■ ASSOCIATED CONTENT

Supporting Information

The Supporting Information is available free of charge at https://pubs.acs.org/doi/10.1021/acscatal.3c04026.

> Fermentation and compound purification conditions; enzymatic reactions under various combinations and under different conditions; NMR data for substrates, substrate analogs, and products from the enzymatic reactions; and additional crystal structural information (PDF)

■ AUTHOR INFORMATION

Corresponding Authors

Lixin Zhang − *State Key Laboratory of Bioreactor Engineering, East China University of Science and Technology, Shanghai 200237, China*; Email: lxzhang@ecust.edu.cn

Wupeng Yan − *School of Life Sciences and Biotechnology, Shanghai Jiao Tong University, Shanghai 200240, China*; Email: yanwupeng@sjtu.edu.cn

Xueting Liu − *State Key Laboratory of Bioreactor Engineering, East China University of Science and Technology, Shanghai 200237, China*; Email: liuxueting@ecust.edu.cn

Pinghua Liu − *Department of Chemistry, Boston University, Boston, Massachusetts 02215, United States*; orcid.org/0000-0002-9768-559X; Email: pinghua@bu.edu

Authors

Xinye Wang − *State Key Laboratory of Bioreactor Engineering, East China University of Science and Technology, Shanghai 200237, China*

Sha Hu − *Department of Chemistry, Boston University, Boston, Massachusetts 02215, United States*

Jun Wang − *School of Life Sciences and Biotechnology, Shanghai Jiao Tong University, Shanghai 200240, China*; orcid.org/0000-0003-2585-5614

Tao Zhang − *Department of Chemistry, Boston University, Boston, Massachusetts 02215, United States*; orcid.org/0000-0002-0715-1739

Ke Ye − *State Key Laboratory of Bioreactor Engineering, East China University of Science and Technology, Shanghai 200237, China*

Aiwen Wen − *Department of Chemistry, Boston University, Boston, Massachusetts 02215, United States*

Guoliang Zhu − *State Key Laboratory of Bioreactor Engineering, East China University of Science and Technology, Shanghai 200237, China*

Arturo Vegas − *Department of Chemistry, Boston University, Boston, Massachusetts 02215, United States*; orcid.org/0000-0001-9522-8208

Complete contact information is available at: https://pubs.acs.org/10.1021/acscatal.3c04026

Author Contributions

#X.W., S.H., J.W., and T.Z. contributed equally to this work. P.L., X.L., W.Y., and L.Z. designed the study. S.H., T.Z., A.W., and X.W. performed biochemical experiments. W.Y., J.W., X.W., and K.Y. performed crystallization and structural determination. P.L., X.L., W.Y., L.Z., G.Z., and A.V. analyzed data and wrote the manuscript with input from all authors. All authors have given approval for the final version of the manuscript.

Funding

This work was supported by the National Key Research and Development Program of China (2019YFA0906201, 2020YFA0907800, 2020YFA090032, 2022YFC2105400), the National Natural Science Foundation of China (32121005, 21977029, 81903529, 32101008, 22307037), the 111 Project (B18022), the Open Project Funding of the State Key Laboratory of Bioreactor Engineering, and the Fundamental Research Funds for the Central Universities. This work is supported in part by the National Institutes of Health (GM140040 to P.L.) and the National Science Foundation (CHE-2004109 to P.L.).

Notes

The authors declare no competing financial interest.

The structure of the $OvoA_{Th2}$·Co^{II}·L-Cys·L-His ternary complex (PDB ID: 8KHQ) can be accessed at https://www.pdbus.org/.

■ ACKNOWLEDGMENTS

The authors thank the staff members at the BL02U1 and BL19U1 beamline at the Shanghai Synchrotron Radiation Facility (SSRF), China, for their assistance in X-ray crystal data collection.

■ REFERENCES

(1) Naowarojna, N.; Cheng, R.; Chen, L.; Quill, M.; Xu, M.; Zhao, C.; Liu, P. Mini-Review: Ergothioneine and Ovothiol Biosyntheses, an Unprecedented Trans-Sulfur Strategy in Natural Product Biosynthesis. *Biochemistry* **2018**, *57* (24), 3309−3325.

(2) Castellano, I.; Seebeck, F. P. On ovothiol biosynthesis and biological roles: from life in the ocean to therapeutic potential. *Nat. Prod. Rep.* **2018**, *35* (12), 1241−1250.

(3) Marjanovic, B.; Simic, M. G.; Jovanovic, S. V. Heterocyclic thiols as antioxidants: why ovothiol C is a better antioxidant than ergothioneine. *Free Radic. Biol. Med.* **1995**, *18* (4), 679−685.

(4) Mirzahosseini, A.; Orgován, G.; Tóth, G.; Hosztafi, S.; Noszál, B. The complete microspeciation of ovothiol A disulfide: a hexabasic symmetric biomolecule. *J. Pharm. Biomed. Anal.* **2015**, *107*, 209−216.
(5) Holler, T. P.; Hopkins, P. B. Ovothiols as biological antioxidants. The thiol groups of ovothiol and glutathione are chemically distinct. *J. Am. Chem. Soc.* **1988**, *110* (14), 4837−4838.
(6) Hand, C. E.; Honek, J. F. Biological chemistry of naturally occurring thiols of microbial and marine origin. *J. Nat. Prod.* **2005**, *68* (2), 293−308.
(7) Russo, G. L.; Russo, M.; Castellano, I.; Napolitano, A.; Palumbo, A. Ovothiol isolated from sea urchin oocytes induces autophagy in the Hep-G2 cell line. *Mar. Drugs* **2014**, *12* (7), 4069−4085.
(8) Holler, T. P.; Hopkins, P. B. Ovothiols as free-radical scavengers and the mechanism of ovothiol-promoted NAD(P)H-O2 oxidoreductase activity. *Biochemistry* **1990**, *29* (7), 1953−1961.
(9) Turner, E.; Klevit, R.; Hager, L. J.; Shapiro, B. M. Ovothiols, a family of redox-active mercaptohistidine compounds from marine invertebrate eggs. *Biochemistry* **1987**, *26* (13), 4028−4036.
(10) Hartman, P. E. Ergothioneine as antioxidant. *Methods Enzymol.* **1990**, *186*, 310−318.
(11) Fahey, R. C. Novel thiols of prokaryotes. *Annu. Rev. Microbiol.* **2001**, *55*, 333−356.
(12) Scott, E. M.; Duncan, I. W.; Ekstrand, V. Purification and properties of glutathione reductase of human erythrocytes. *J. Biol. Chem.* **1963**, *238* (12), 3928−3933.
(13) Aruoma, O. I.; Whiteman, M.; England, T. G.; Halliwell, B. Antioxidant action of ergothioneine: assessment of its ability to scavenge peroxynitrite. *Biochem. Biophys. Res. Commun.* **1997**, *231* (2), 389−391.
(14) Franzoni, F.; Colognato, R.; Galetta, F.; Laurenza, I.; Barsotti, M.; Di Stefano, R.; Bocchetti, R.; Regoli, F.; Carpi, A.; Balbarini, A. An *in vitro* study on the free radical scavenging capacity of ergothioneine: comparison with reduced glutathione, uric acid and trolox. *Biomed. Pharmacother.* **2006**, *60* (8), 453−457.
(15) Jang, J.-H.; Aruoma, O. I.; Jen, L.-S.; Chung, H. Y.; Surh, Y.-J. Ergothioneine rescues PC12 cells from β-amyloid-induced apoptotic death. *Free Radic. Biol. Med.* **2004**, *36* (3), 288−299.
(16) Taubert, D.; Lazar, A.; Grimberg, G.; Jung, N.; Rubbert, A.; Delank, K.-S.; Perniok, A.; Erdmann, E.; Schömig, E. Association of rheumatoid arthritis with ergothioneine levels in red blood cells: a case control study. *J. Rheumatol.* **2006**, *33* (11), 2139−2145.
(17) Tokuhiro, S.; Yamada, R.; Chang, X.; Suzuki, A.; Kochi, Y.; Sawada, T.; Suzuki, M.; Nagasaki, M.; Ohtsuki, M.; Ono, M.; Furukawa, H.; Nagashima, M.; Yoshino, S.; Mabuchi, A.; Sekine, A.; Saito, S.; Takahashi, A.; Tsunoda, T.; Nakamura, Y.; Yamamoto, K. An intronic SNP in a RUNX1 binding site of SLC22A4, encoding an organic cation transporter, is associated with rheumatoid arthritis. *Nat. Genet.* **2003**, *35* (4), 341−348.
(18) Peltekova, V. D.; Wintle, R. F.; Rubin, L. A.; Amos, C. I.; Huang, Q.; Gu, X.; Newman, B.; Van Oene, M.; Cescon, D.; Greenberg, G.; Griffiths, A. M.; St George-Hyslop, P. H.; Siminovitch, K. A. Functional variants of OCTN cation transporter genes are associated with Crohn disease. *Nat. Genet.* **2004**, *36* (5), 471−475.
(19) Leung, E.; Hong, J.; Fraser, A. G.; Merriman, T. R.; Vishnu, P.; Krissansen, G. W. Polymorphisms in the organic cation transporter genes SLC22A4 and SLC22A5 and Crohn's disease in a New Zealand Caucasian cohort. *Immunol. Cell Biol.* **2006**, *84* (2), 233−236.
(20) Kaneko, I.; Takeuchi, Y.; Yamaoka, Y.; Tanaka, Y.; Fukuda, T.; Fukumori, Y.; Mayumi, T.; Hama, T. Quantitative determination of ergothioneine in plasma and tissues by TLC-densitometry. *Chem. Pharm. Bull.* **1980**, *28* (10), 3093−3097.
(21) Briggs, I. Ergothioneine in the central nervous system. *J. Neurobiochem.* **1972**, *19* (1), 27−35.
(22) Crossland, J.; Mitchell, J.; Woodruff, G. N. The presence of ergothioneine in the central nervous system and its probable identity with the cerebellar factor. *J. Physiol.* **1966**, *182* (2), 427−438.
(23) Moncaster, J. A.; Walsh, D. T.; Gentleman, S. M.; Jen, L.-S.; Aruoma, O. I. Ergothioneine treatment protects neurons against N-methyl-D-aspartate excitotoxicity in an *in vivo* rat retinal model. *Neurosci. Lett.* **2002**, *328* (1), 55−59.
(24) Libby, P.; Ridker, P. M.; Hansson, G. K. Progress and challenges in translating the biology of atherosclerosis. *Nature* **2011**, *473* (7347), 317−325.
(25) Bastard, J.-P.; Maachi, M.; Van Nhieu, J. T.; Jardel, C.; Bruckert, E.; Grimaldi, A.; Robert, J.-J.; Capeau, J.; Hainque, B. Adipose tissue IL-6 content correlates with resistance to insulin activation of glucose uptake both in vivo and in vitro. *J. Clin. Endocrinol. Metab.* **2002**, *87* (5), 2084−2089.
(26) Cheah, I. K.; Halliwell, B. Ergothioneine; antioxidant potential, physiological function and role in disease. *Biochim. Biophys. Acta* **2012**, *1822* (5), 784−793.
(27) Cheah, I. K.; Halliwell, B. Could ergothioneine aid in the treatment of coronavirus patients? *Antioxidants (Basel)* **2020**, *9* (7), 595.
(28) Ames, B. N. Prolonging healthy aging: longevity vitamins and proteins. *Proc. Natl. Acad. Sci. U. S. A.* **2018**, *115* (43), 10836−10844.
(29) Steele, A. D.; Kiefer, A. F.; Shen, B. The many facets of sulfur incorporation in natural product biosynthesis. *Curr. Opin. Chem. Biol.* **2023**, *76*, No. 102366.
(30) Dunbar, K. L.; Scharf, D. H.; Litomska, A.; Hertweck, C. Enzymatic carbon-sulfur bond formation in natural product biosynthesis. *Chem. Rev.* **2017**, *117* (8), 5521−5577.
(31) Mahanta, N.; Szantai-Kis, D. M.; Petersson, E. J.; Mitchell, D. A. Biosynthesis and chemical applications of thioamides. *ACS Chem. Biol.* **2019**, *14* (2), 142−163.
(32) Burkhart, B. J.; Schwalen, C. J.; Mann, G.; Naismith, J. H.; Mitchell, D. A. YcaO-dependent posttranslational amide activation: biosynthesis, structure, and function. *Chem. Rev.* **2017**, *117* (8), 5389−5456.
(33) Reich, H. J.; Hondal, R. J. Why Nature chose selenium. *ACS Chem. Biol.* **2016**, *11* (4), 821−841.
(34) Kayrouz, C. M.; Huang, J.; Hauser, N.; Seyedsayamdost, M. R. Biosynthesis of selenium-containing small molecules in diverse microorganisms. *Nature* **2022**, *610* (7930), 199−204.
(35) Cheng, R.; Lai, R.; Peng, C.; Lopez, J.; Li, Z.; Naowarojna, N.; Li, K.; Wong, C.; Lee, N.; Whelan, S. A.; Qiao, L.; Grinstaff, M. W.; Wang, J.; Cui, Q.; Liu, P. Implications for an imidazol-2-yl carbene intermediate in the rhodanase-catalyzed C-S bond formation reaction of anaerobic ergothioneine biosynthesis. *ACS Catal.* **2021**, *11* (6), 3319−3334.
(36) Chen, X.; Li, B. How nature incorporates sulfur and selenium into bioactive natural products. *Curr. Opin. Chem. Biol.* **2023**, *76*, No. 102377.
(37) Seebeck, F. P. In vitro reconstitution of Mycobacterial ergothioneine biosynthesis. *J. Am. Chem. Soc.* **2010**, *132* (19), 6632−6633.
(38) Song, H.; Hu, W.; Naowarojna, N.; Her, A. S.; Wang, S.; Desai, R.; Qin, L.; Chen, X.; Liu, P. Mechanistic studies of a novel C-S lyase in ergothioneine biosynthesis: the involvement of a sulfenic acid intermediate. *Sci. Rep.* **2015**, *5*, 11870.
(39) Hu, W.; Song, H.; Sae Her, A.; Bak, D. W.; Naowarojna, N.; Elliott, S. J.; Qin, L.; Chen, X.; Liu, P. Bioinformatic and biochemical characterizations of C-S bond formation and cleavage enzymes in the fungus *Neurospora crassa* ergothioneine biosynthetic pathway. *Org. Lett.* **2014**, *16* (20), 5382−5385.
(40) Irani, S.; Naowarojna, N.; Tang, Y.; Kathuria, K. R.; Wang, S.; Dhembi, A.; Lee, N.; Yan, W.; Lyu, H.; Costello, C. E.; Liu, P.; Zhang, Y. J. Snapshots of C-S cleavage in Egt2 reveals substrate specificity and reaction mechanism. *Cell Chem. Biol.* **2018**, *25* (5), 519−529.e4.
(41) Burn, R.; Misson, L.; Meury, M.; Seebeck, F. P. Anaerobic origin of ergothioneine. *Angew. Chem., Int. Ed.* **2017**, *56* (41), 12508−12511.
(42) Cheng, R.; Wu, L.; Lai, R.; Peng, C.; Naowarojna, N.; Hu, W.; Li, X.; Whelan, S. A.; Lee, N.; Lopez, J.; Zhao, C.; Yong, Y.; Xue, J.; Jiang, X.; Grinstaff, M. W.; Deng, Z.; Chen, J.; Cui, Q.; Zhou, J.; Liu, P. Single-step replacement of an unreactive C-H bond by a C-S bond

https://doi.org/10.1021/acscatal.3c04026
ACS Catal. 2023, 13, 15417−15426

using polysulfide as the direct sulfur source in anaerobic ergothioneine biosynthesis. *ACS Catal.* **2020**, *10* (16), 8981−8994.
(43) Beliaeva, M. A.; Seebeck, F. P. Discovery and characterization of the metallopterin-dependent ergothioneine synthase from *Caldithrix abyssi*. *JACS Au* **2022**, *2* (9), 2098−2107.
(44) Braunshausen, A.; Seebeck, F. P. Identification and characterization of the first ovothiol biosynthetic enzyme. *J. Am. Chem. Soc.* **2011**, *133* (6), 1757−1759.
(45) Naowarojna, N.; Huang, P.; Cai, Y.; Song, H.; Wu, L.; Cheng, R.; Li, Y.; Wang, S.; Lyu, H.; Zhang, L.; Zhou, J.; Liu, P. *In vitro* reconstitution of the remaining steps in ovothiol A biosynthesis: C−S lyase and methyltransferase reactions. *Org. Lett.* **2018**, *20* (17), 5427−5430.
(46) Song, H.; Leninger, M.; Lee, N.; Liu, P. Regioselectivity of the oxidative C-S bond formation in ergothioneine and ovothiol biosyntheses. *Org. Lett.* **2013**, *15* (18), 4854−4857.
(47) Goncharenko, K. V.; Vit, A.; Blankenfeldt, W.; Seebeck, F. P. Structure of the sulfoxide synthase EgtB from the ergothioneine biosynthetic pathway. *Angew. Chem., Int. Ed.* **2015**, *54* (9), 2821−2824.
(48) Naowarojna, N.; Irani, S.; Hu, W.; Cheng, R.; Zhang, L.; Li, X.; Chen, J.; Zhang, Y. J.; Liu, P. Crystal Structure of the ergothioneine sulfoxide synthase from *Candidatus* chloracidobacterium thermophilum and structure-guided engineering to modulate its substrate selectivity. *ACS Catal.* **2019**, *9* (8), 6955−6961.
(49) Stampfli, A. R.; Goncharenko, K. V.; Meury, M.; Dubey, B. N.; Schirmer, T.; Seebeck, F. P. An alternative active site architecture for O_2 activation in the ergothioneine biosynthetic EgtB from *Chloracidobacterium thermophilum*. *J. Am. Chem. Soc.* **2019**, *141* (13), 5275−5285.
(50) Chen, L.; Naowarojna, N.; Song, H.; Wang, S.; Wang, J.; Deng, Z.; Zhao, C.; Liu, P. Use of a tyrosine analogue to modulate the two activities of a nonheme iron enzyme OvoA in ovothiol biosynthesis, cysteine oxidation versus oxidative C-S bond formation. *J. Am. Chem. Soc.* **2018**, *140* (13), 4604−4612.
(51) Chen, L.; Naowarojna, N.; Chen, B.; Xu, M.; Quill, M.; Wang, J.; Deng, Z.; Zhao, C.; Liu, P. Mechanistic studies of a nonheme iron enzyme OvoA in ovothiol biosynthesis using a tyrosine analogue, 2-amino-3-(4-hydroxy-3-(methoxyl) phenyl) propanoic acid (MeO-Tyr). *ACS Catal.* **2019**, *9*, 253−258.
(52) Cheng, R.; Weitz, A. C.; Paris, J.; Tang, Y.; Zhang, J.; Song, H.; Naowarojna, N.; Li, K.; Qiao, L.; Lopez, J.; Grinstaff, M. W.; Zhang, L.; Guo, Y.; Elliott, S.; Liu, P. OvoA(Mtht) from *Methyloversatilis thermotolerans* ovothiol biosynthesis is a bifunction enzyme: thiol oxygenase and sulfoxide synthase activities. *Chem. Sci.* **2022**, *13* (12), 3589−3598.
(53) Shannon, P.; Markiel, A.; Ozier, O.; Baliga, N. S.; Wang, J. T.; Ramage, D.; Amin, N.; Schwikowski, B.; Ideker, T. Cytoscape: a software environment for integrated models of biomolecular interaction networks. *Genome Res.* **2003**, *13* (11), 2498−504.
(54) Takai, K.; Nealson, K. H.; Horikoshi, K. *Hydrogenimonas thermophila* gen. nov., sp. nov., a novel thermophilic, hydrogen-oxidizing chemolithoautotroph within the epsilon-*Proteobacteria*, isolated from a black smoker in a Central Indian Ridge hydrothermal field. *Int. J. Syst. Evol. Microbiol.* **2004**, *54* (Pt 1), 25−32.
(55) Wen, J.; Lord, H.; Knutson, N.; Wikstrom, M. Nano differential scanning fluorimetry for comparability studies of therapeutic proteins. *Anal. Biochem.* **2020**, *593*, No. 113581.
(56) Kim, S. H.; Yoo, H. J.; Park, E. J.; Na, D. H. Nano differential scanning fluorimetry-based thermal stability screening and optimal buffer selection for immunoglobulin G. *Pharmaceuticals (Basel)* **2022**, *15* (1), 29.
(57) Song, H.; Her, A. S.; Raso, F.; Zhen, Z.; Huo, Y.; Liu, P. Cysteine oxidation reactions catalyzed by a mononuclear non-heme iron enzyme (OvoA) in ovothiol biosynthesis. *Org. Lett.* **2014**, *16* (8), 2122−2125.
(58) Krissinel, E.; Henrick, K. Inference of macromolecular assemblies from crystalline state. *J. Mol. Biol.* **2007**, *372* (3), 774−97.
(59) Gao, S. S.; Naowarojna, N.; Cheng, R.; Liu, X.; Liu, P. Recent examples of alpha-ketoglutarate-dependent mononuclear non-haem iron enzymes in natural product biosyntheses. *Nat. Prod. Rep.* **2018**, *35* (8), 792−837.
(60) Goncharenko, K. V.; Seebeck, F. P. Conversion of a non-heme iron-dependent sulfoxide synthase into a thiol dioxygenase by a single point mutation. *Chem. Commun.* **2016**, *52* (9), 1945−1948.
(61) Paris, J. C.; Hu, S.; Wen, A.; Weitz, A. C.; Cheng, R.; Gee, L. B.; Tang, Y.; Kim, H.; Vegas, A.; Chang, W. C.; Elliott, S. J.; Liu, P.; Guo, Y. An S = 1 Iron(IV) intermediate revealed in a non-heme iron enzyme-catalyzed oxidative C-S bond formation. *Angew. Chem., Int. Ed.* **2023**, *62*, No. e202309362.
(62) Ziemert, N.; Alanjary, M.; Weber, T. The evolution of genome mining in microbes - a review. *Nat. Prod. Rep.* **2016**, *33* (8), 988−1005.
(63) Pan, G.; Xu, Z.; Guo, Z.; Hindra; Ma, M.; Yang, D.; Zhou, H.; Gansemans, Y.; Zhu, X.; Huang, Y.; Zhao, L. X.; Jiang, Y.; Cheng, J.; Van Nieuwerburgh, F.; Suh, J. W.; Duan, Y.; Shen, B. Discovery of the leinamycin family of natural products by mining actinobacterial genomes. *Proc. Natl. Acad. Sci. U. S. A.* **2017**, *114* (52), E11131−E11140.
(64) Sasaki, E.; Zhang, X.; Sun, H. G.; Lu, M. Y.; Liu, T. L.; Ou, A.; Li, J. Y.; Chen, Y. H.; Ealick, S. E.; Liu, H. W. Co-opting sulphur-carrier proteins from primary metabolic pathways for 2-thiosugar biosynthesis. *Nature* **2014**, *510* (7505), 427−431.
(65) Zhang, X.; Xu, X.; You, C.; Yang, C.; Guo, J.; Sang, M.; Geng, C.; Cheng, F.; Du, L.; Shen, Y.; Wang, S.; Lan, H.; Yang, F.; Li, Y.; Tang, Y. J.; Zhang, Y.; Bian, X.; Li, S.; Zhang, W. Biosynthesis of chuangxinmycin featuring a deubiquitinase-like sulfurtransferase. *Angew. Chem., Int. Ed.* **2021**, *60* (46), 24418−24423.
(66) Krishnamoorthy, K.; Begley, T. P. Protein thiocarboxylate-dependent methionine biosynthesis in *Wolinella succinogenes*. *J. Am. Chem. Soc.* **2011**, *133* (2), 379−386.
(67) Dahiya, R.; Dahiya, S.; Fuloria, N. K.; Kumar, S.; Mourya, R.; Chennupati, S. V.; Jankie, S.; Gautam, H.; Singh, S.; Karan, S. K.; Maharaj, S.; Fuloria, S.; Shrivastava, J.; Agarwal, A.; Singh, S.; Kishor, A.; Jadon, G.; Sharma, A. Natural bioactive thiazole-based peptides from marine resources: structural and pharmacological aspects. *Mar. Drugs* **2020**, *18* (6), 329.
(68) Tanaka, N.; Kawano, Y.; Satoh, Y.; Dairi, T.; Ohtsu, I. Gram-scale fermentative production of ergothioneine driven by overproduction of cysteine in *Escherichia coli*. *Sci. Rep.* **2019**, *9* (1), 1895.

https://doi.org/10.1021/acscatal.3c04026
ACS Catal. 2023, 13, 15417−15426